CONTROL OF DRAG REDUCTION OF FUNCTIONAL FLUID FLOW IN RECTANGULAR CHANNEL - SPATIAL STRUCTURE AND RECOVERY PROCESS OF TURBULENCE INVESTIGATED BY PIV -

Yasuo KAWAGUCHI, Ziping FENG[1]
National Institute of Advanced Industrial Science and Technology
1-2 Namiki, Tsukuba, 305-8564 Japan
m4050@mel.go.jp
1:Center for Smart Control of Turbulence

Peiwen LI
Dept. Mech. Eng., Kyoto University
Yoshida-Honmachi, Sakyo-ku, Kyoto, 606-8501 Japan
lipeiwen@mech.kyoto-u.ac.jp

ABSTRACT
The turbulent frictional drag of water can be reduced dramatically by adding small amounts of drag-reducing materials, such as polymers or surfactants. As a percentage drag reduction of 80% can easily be achieved, this technique is thought to be the most practical method of reducing turbulent frictional drag.
In this work, a double pulse PIV system was used to clarify the spatial velocity distribution of surfactant solution flow in a two-dimensional channel. A type of cationic surfactant CTAC ($C_{16}H_{33}N(CH_3)_3Cl$) mixed with the same weight of counter-ion material NaSal (HOC_6H_4COONa) was used as a drag-reducing additive to water at a mass concentration of 40 ppm. Instantaneous velocity distribution taken by PIV was examined to clarify the effect of surfactant additives as well as recovery behavior of drag-reducing flow in a narrowed channel.

1. INTRODUCTION
Since the discovery of Tom's effect (Mysels, 1949; Toms, 1948), the reduction of turbulent skin friction by adding drag-reducing materials has received drag-reducing additives for turbulent water flow to reduce the frictional drag by up to 80%. However, polymer solutions are strongly affected by increasing attention for conserving pumping power in fluid transportation. Polymers were initially used as mechanical degradation, which may result in shorter lifetime of drag reduction effectiveness. Surfactants were found in the last two decades also to reduce the frictional drag by 70% to 80% but to be less affected by mechanical degradation (Ohlendorf et al., 1986; Bewersdorff et al., 1988). Therefore, surfactants are now being considered as practical drag-reducing additives.
A recent application of drag-reducing additives is to reduce the pumping power in district heating and cooling systems where cationic surfactants are used in closed circuits (Gyr and Bewersdorff, 1995; Gasljevic and Matthys, 1997; Pollert et al., 1994).

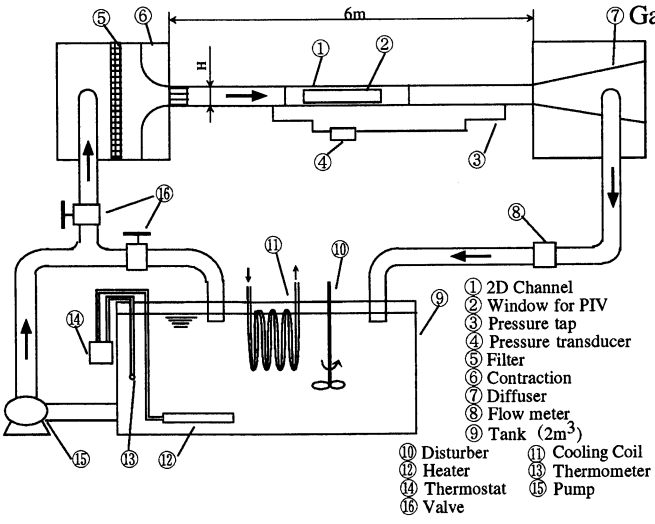

Figure 1: Schematic diagram of two dimensional water channel

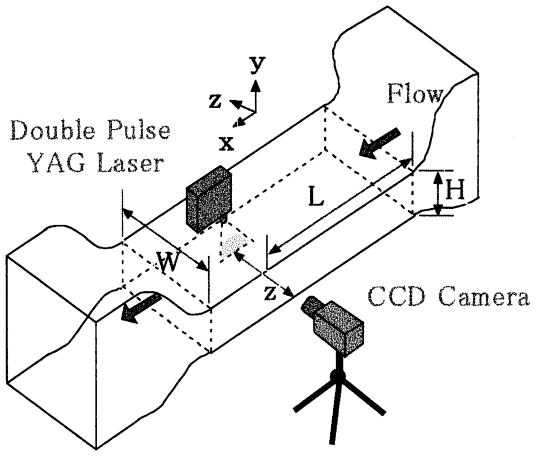

Figure 2 : Schematic view of PIV arrangement

The authors are continuing experimental studies on drag reduction phenomena in order to optimize district heating and cooling systems (Kawaguchi et al., 1996, 1997a, 1997b). Kawaguchi et al. (1996) carried out an investigation on how the turbulent characteristics in a two-dimensional channel are modified by surfactant additives by using a two-component LDV system, and discussed the effect of surfactant concentration and Reynolds number. In this paper, PIV was employed to investigate the spatial structure of drag-reducing flow. The transitional behavior of the flow in a narrowed channel will be also discussed.

2. EXPERIMENTAL APPARATUS AND PROCEDURE

2.1 Water channel

The present experiments were carried out in a closed liquid flow loop, which is shown in Figure 1. The system consists of a reservoir tank, a pump, a settling chamber equipped with a nozzle, a two-dimensional channel, a diffuser and an electro-magnetic flow meter. The test section is equipped with glass windows at several locations and is 40 mm high (H), 500 mm wide (W) and 6 m long (inside measurements). Most of the test section is made of transparent acrylic resin having a thickness of 20 mm. The surfactant aqueous solution is circulated by the pump and supplied to the settling chamber, which is equipped with a perforated pipe, stainless steel mesh and 1/12.5 contraction nozzle. At the entrance of the test section, a honeycomb of 150 mm length having 10 mm by 10 mm rectangular openings was used to remove large eddies. The PIV measurement position (L) is 5000 mm (=125H) downstream from the inlet of the test section. For measurements of pressure drop, a high-precision differential pressure meter was used. The reading provided by the flow meter and the flow rate calculated from the velocity profile measured by LDV coincided within 3%.

2.2 PIV system

The PIV measurement system arranged by TSI consists of a double pulse laser, laser sheet optics, CCD camera, timing circuit, PC and software. The system can take pictures of particles at a resolution of 1008 by 1018 pixels and transfer images to the computer at the rate of 30 frames per second. TSI's Insight ver. 2.01 software was used for data processing. As the generation of error vectors caused by imperfection in the optical system or software was unavoidable, a special Fortran program was written for eliminating the error vectors and performing statistical calculation based on the acquired vector distribution.

The arrangement of the water channel and PIV system are shown in Fig. 2. Cartesian coordinates are also shown in the diagram. According to common usage, the x, y and z coordinates are aligned to the stream direction, normal to the bottom wall and spanwise direction respectively. Most of the picture frames (40 mm by 34 mm) were taken to cover the full height of the channel. Fine particles (Vestosint, Degussa) were used as scattering particles, with nominal particle diameter of 60 μm, and density of 1.03g/cm^3 The concentration of particles was carefully controlled to show clear PIV pictures.

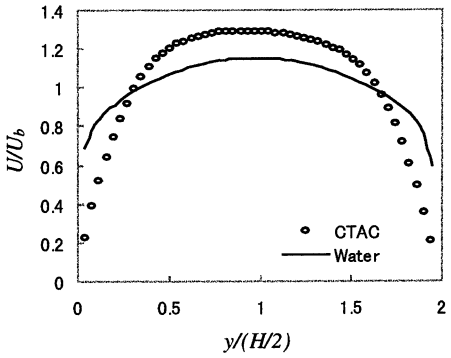

Figure 3 : Mean velocity profiles at Re=21000 (line: water, symbol: CTAC 40ppm)

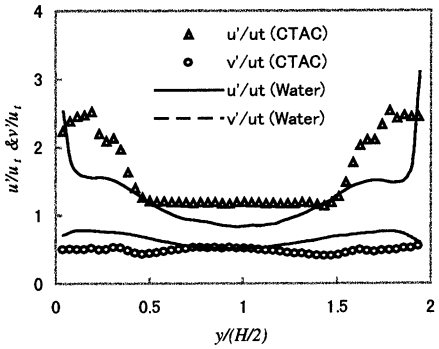

Figure 4 : Distribution of turbulent Intensities at Re=21000 (line: water, symbol: CTAC 40ppm)

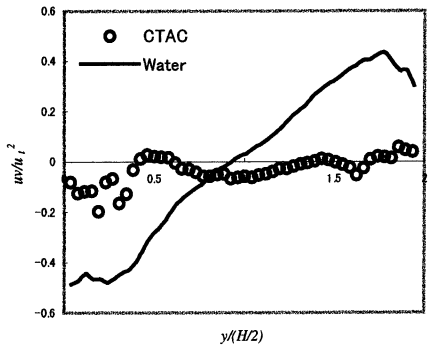

Figure 5 : Distribution of Reynolds shear stress at Re=21000 (line: water, symbol: CTAC 40ppm)

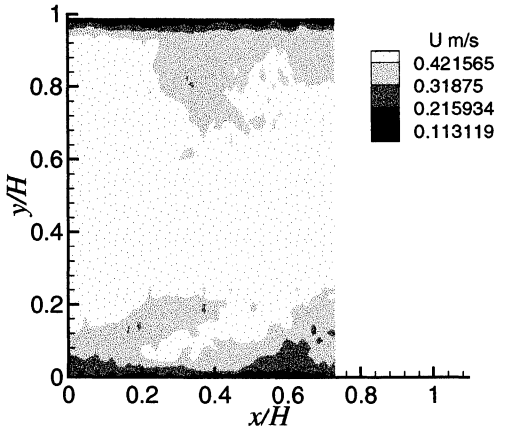

Figure 6a : Instantaneous velocity distribution in drag-reducing flow (CTAC 40ppm) at Re=21000

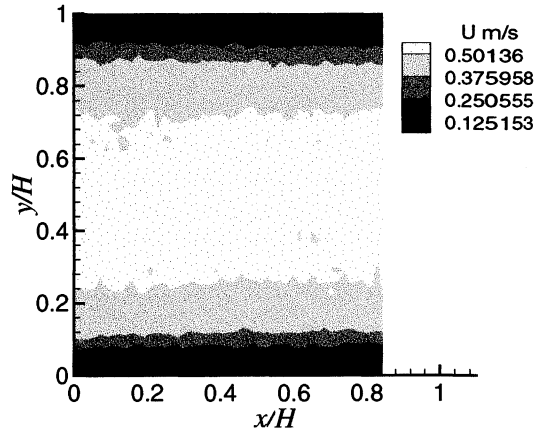

Figure 6b : Instantaneous velocity distribution in drag-reducing flow (CTAC 40ppm) at Re=21000

2.3 Surfactant solution

The surfactant solution used in this study was cetyltrimethyl ammonium chloride (CTAC), which has the chemical formula of $C_{16}H_{33}N(CH_3)_3Cl$, dissolved in tap water. CTAC is a cationic surfactant that is known to be very effective for drag reduction when accompanied with a suitable organic salt such as sodium salicylate (NaSal, HOC_6H_4COONa).

3. RESULTS AND DISCUSSION

3.1 Effect of surfactant additives on mean velocity and statistical quantities of turbulent velocity fluctuation

Prior to the PIV measurement, the friction factor was experimentally determined for water with and without surfactant additives. The largest percentage of drag reduction in this experiment was around 60%. The mean velocity profile was determined based on 500 frames of instantaneous velocity distribution taken by PIV.

The obtained mean velocity (U) profiles with and without surfactant are shown in Fig. 3, where lines represent the velocity profiles for water at each Reynolds number. Bulk mean velocity U_b was used for normalization. It is well known that the velocity profiles for water are roughly correlated by the 1/n power law. In this Reynolds number range, mean velocity near the centerline of the channel becomes flat and the velocity gradient near the wall is large. In contrast, velocity profile for surfactant solution show a steeper peak near the centerline, indicating that the mean velocity gradient near the wall of the surfactant solution is lower than that of the water flow. This finding corresponds to the result obtained by LDV (Kawaguchi et al. 1996) that the velocity profile of drag-reducing flow approaches to but does not coincide to laminar-like velocity profile.

Figure 4 compares intensities of turbulent fluctuation normalized by frictional velocity u_t As previously reported in the study using LDV, turbulence fluctuations normalized by frictional velocity are not largely suppressed. The location of the peak in u' distribution shifts outward from the wall in the surfactant case. The distribution of v' shows that slight suppression occurs when surfactant is added to the water.

Figure 5 shows the Reynolds shear stress (uv) profile in the water channel. The result is surprising because aside from the scatter in y of less than y/H=0.5, the crosscorrelation of u and v becomes almost zero in drag-reducing flow. As the two components of normal stress have finite values, the absence of Reynolds shear stress comes from de-correlation of the two components of velocity fluctuation.

3.2 Effect of surfactant additives on spatial distribution of instantaneous velocity and length scale

This section discusses the instantaneous spatial velocity distribution at Re=21000 taken by PIV with and without surfactant additives. Figure 6a shows the contour map based on the magnitude of velocity. In the figure, the main flow direction is from left to right and the frame covers the full height of the channel. The figure shows a random pattern of complicated ridges, valleys and peaks near the channel wall. This means large velocity fluctuations in time and space occupy this field. Near the bottom wall, there is an inclined structure of the low velocity region penetrating the high velocity region. One interesting finding from the colored contour is the existence of acceleration or deceleration fronts near the wall. The acceleration front starts from the location of (x, y) = (15 mm, 1 mm) and reaches to (5 mm, 7 mm). This front inclines downward and has an angle of about 30 deg. In the region near the wall, contour lines are closely distributed, reflecting the large velocity gradient near the wall which is commonly seen in turbulent wall flow.

Figure 6b shows the instantaneous velocity distribution taken in CTAC 30ppm solution. As seen in the figure, the flow differs from that without surfactant. The complicated ridge and valley pattern and acceleration or deceleration front disappear. Velocity gradient near the wall becomes smaller.

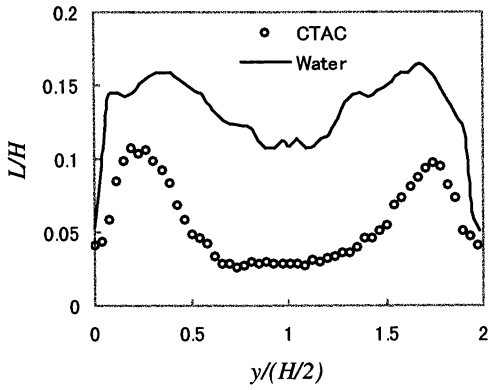

Figure 7 : Distribution of intergal length scale of *u'*

The spatial pattern of the instantaneous velocity suggests that the large coherent motion in water flow disappears in surfactant solution flow. The lack of large-scale motion may shorten the length scale of turbulent fluctuation. Figure 7 shows the calculated result of integral length scale in the *x* direction based on the autocorrelation of *u*. The length scale *L* near the wall increases proportionally with the increase of *y* and it becomes around 0.12 of channel height *H* in the core region of the channel. In CTAC solution, the length scale is much smaller than that in water, thus supporting the idea of lower turbulent diffusivity and lower drag observed in surfactant solution flows.

3.3 Effect of surfactant additives on instantaneous spatial distribution of vorticity and vorticity related quantities

Corresponding to the velocity fluctuation, vorticity fluctuation is also affected by surfactant additives. Figures 8a and 8b compare vorticity fluctuation ω_z with and without surfactant additives, calculated from the common data demonstrated in Figures 6a and 6b respectively. Note that contour lines are drawn to divide the range defined by minimum and maximum values appearing in the frame. These values are designated in each figure. As shown in Fig. 8a, large positive and negative vorticities were observed around the observed front near the wall in Fig. 6a. In comparison, surfactant additives suppress violent vorticity motion as seen in Fig. 6b. Vorticity fluctuation is relatively weak and evenly distributed. The spatial scale of vorticity fluctuation seems small and corresponds to smaller length scale as discussed in the previous section.

Kevlahan (1993) proposed the classification of turbulent structure based on the parameter $\Sigma=(S^2_{ij}-\Omega^2_{ij})/(S^2_{ij}+\Omega^2_{ij})$ where S_{ij} represents strain tensor and Ω_{ij} vorticity tensor. Kevlahan classified five basic structure types defined by the value of Σ and pressure. In this study, as the pressure is unknown, the following four types were determined based on Σ, S, Ω.

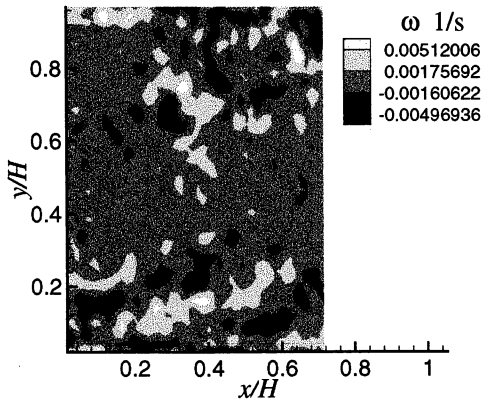

Figure 8a : Vorticity fluctuation distribution in water flow (CTAC 0 ppm) at Re=21000

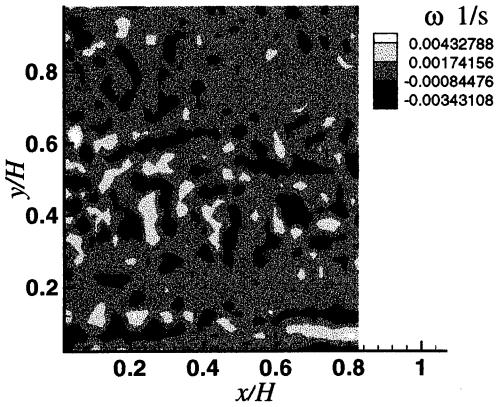

Figure 8b : Vorticity fluctuation distribution in drag-reducing flow (CTAC 40 ppm) at Re=21000

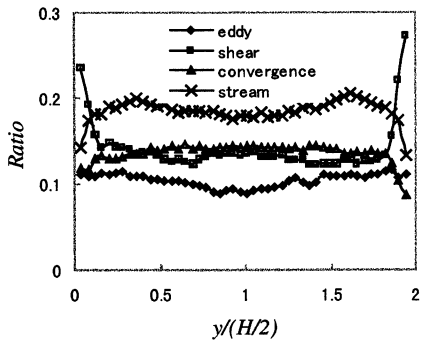

Figure 9a : Ratio of probability of classified structure in water flow (CTAC 0 ppm) at Re=21000

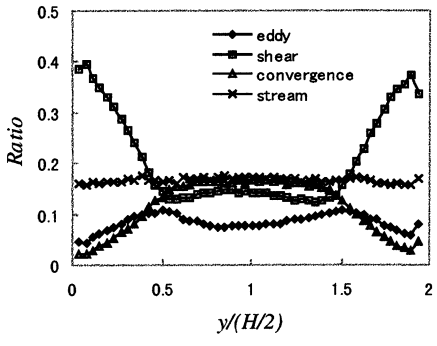

Figure 9b : Ratio of probability of classified structure in drag-reducing flow (40ppm) at Re=21000

"Eddies": $|\Omega| > \Omega'$, $|\Sigma| > \Sigma'$ and $\Sigma < -1/3$,
"Shear": $|\Omega| > \Omega'$, $|\Sigma| > \Sigma'$ and $-1/3 < \Sigma < 1/3$,
"Convergence": $|\Omega| > \Omega'$, $|\Sigma| > \Sigma'$ and $\Sigma > 1/3$,
"Streaming": $|\Omega| < \Omega'$, $|\Sigma| < \Sigma'$ and $|u| > u'$

"Eddies" are regions of high vorticity, "Shear" structures are regions of shear strain, "Convergence" structures are regions of irrotational strain characterized by converging streamlines, and "Streaming" structures are regions of low deformation and high kinetic energy. Kevlahan applied this classification to analyze the DNS result of distorting turbulence. This classification is also applicable to experimental data of PIV. Figures 9a and 9b shows the distribution of probability of these four structures. In water channel flow shown in Figure 6a, "Streaming" is the largest contributor in most of the channel. Only in the thin layer near the wall, the probability of "Shear" structures becomes the largest. In contrast, surfactant solution flow has a thick layer characterized by "Shear" structures. In such layer, the probabilities of "Eddies" and "Convergence" structures become small.

3.4 Transitional behavior of drag reducing flow in narrowed channel

The control of drag reduction, which means temporary termination of drag reduction, is also an important issue for industrial application of this technology.

It is generally believed that the aggregated macro-scale structure of surfactant molecules in water is causes drag reduction phenomena. The structure gives non-Newtonian fluid properties to the solution which effectively suppress turbulence. The structure can be degraded by large shear deformation in which case the effectiveness of turbulent is lost. Therefore, when we apply excess shear to the fluid, the flow turns laminar and the turbulence suppressed state suddenly switches to the ordinary turbulent state. By this principle, we can manipulate turbulent drag in the range of 20% to 100% of that of water flow at the same Reynolds number.

To increase wall shear stress at constant Re, we installed a narrowed channel as shown in Figure 10. In this test section, the drag-reducing flow was designed to introduce the flow into a contracted channel where a high local shear stress can be exerted to the flow in order to have temporary degradation of drag reduction. The transitional turbulence and local heat transfer characteristics in the contracted channel were reported by the authors (Li, Kawaguchi and Yabe, 1999), in which LDV was used to measure turbulent properties. To clarify the instantaneous structure of the transitional flow, the PIV system was used and the spatial vortex motion is reported in this work.

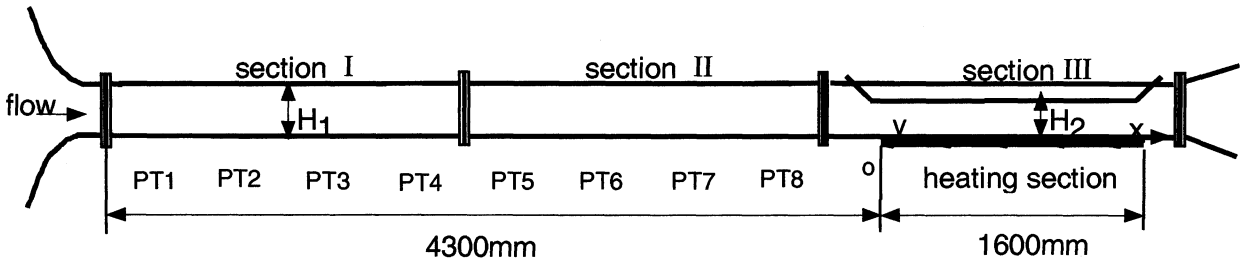

Figure 10 : Schematic diagram of narrowed channel installed in the flow loop

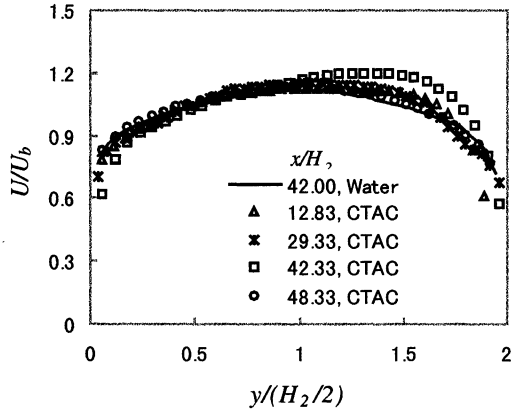

Figure 11 : Mean velocity profile at different x positions in Narrowed channel, Re=46000

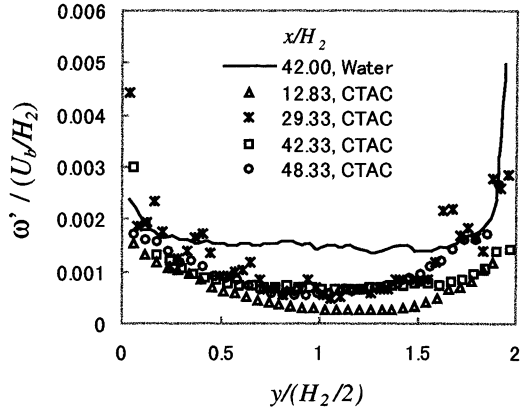

Figure 12 : Intensity of vorticity fluctuation at different x positions in Narrowed channel, Re=46000

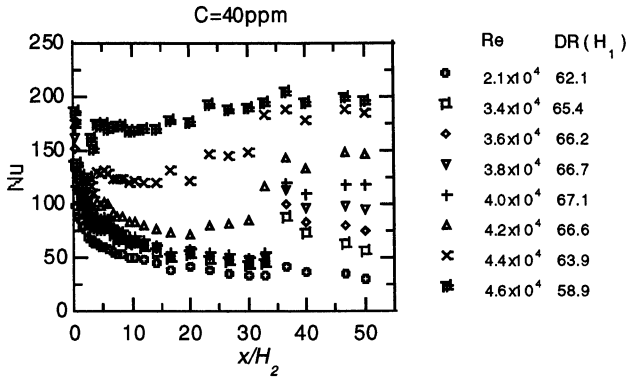

Figure 13 : Local heat transfer coefficient in the entdrance region of narrowed channel (Li et al. 1999)

Figures 11 and 12 show mean velocity profiles and intensity of vorticity fluctuation at several locations from the inlet of the narrowed channel. Figure 13 shows the local heat transfer coefficient measured in the narrowed channel. The heat transfer distribution starts from a lower level, which corresponds to lower diffusivity and low skin friction. With increase of x, the heat transfer coefficient gradually increases and reaches the level of water flow without drag-reducing additives. This trend suggests that the recovery of heat transfer requires a certain recovery time. In contrast, the velocity profiles and turbulent intensities shown in Figures 11 and 12 have been recovered at an early stage. Then, at the entrance of the channel, there exists the normal turbulent velocity field but lower thermal diffusivity.

The finding of such an inconsistency is interesting from the view of controlling drag reduction phenomena. The velocity fluctuation observed near the wall has similar characteristics as that in ordinary turbulence. Kawaguchi et al. (1997a) also investigated the thermal boundary layer in drag-reducing flow and found double diffusivity layers. This can be explained by the present observation that flow can be unstable in the near-wall region but still be stable drag-reducing flow in the outer layer.

4. CONCLUSIONS

The following conclusions were drawn from the present study.

1. The instantaneous velocity distribution taken in water flow exhibits penetration from the low-speed fluid region into the high-speed region, which is one of the important events of turbulence energy production and turbulent mixing. Although this structure is commonly observed in water flow, it was not found in drag-reducing flow under the same Reynolds number.

2. The strong vorticity fluctuation near the wall also disappears and the integral length scale of turbulent fluctuation has a smaller value in surfactant solution flow.

3. The heat transfer coefficient recovers in the narrowed channel but does not accompany the recovery of velocity field. Further study is needed to clarify the reason for this inconsistency between thermal and flow fields.

Acknowledgments

This research was carried out as a research project of the Center for Smart Control of Turbulence with the financial support by the Ministry of Education, Culture, Sports, Science and Technology (MECSST).

REFERENCES

Bewersdorff, H.-W. and Ohlendorf, D., 1988, "The Behavior of Drag-Reducing Cationic Surfactants", J. Colloid and Polymer Science, Vol. 266, No. 10, pp. 941-953.

Gasljevic, K. and Matthys, E.F., 1996, "Field Test of a Drag-Reducing Surfactant Additives in a Hydraulic Cooling System", ASME FED-Vol. 237, pp. 249-260.

Gyr, A. and Bewersdorff, H.-W., 1995, "Drag Reduction of Turbulent Flows by Additives", Kluwer Academic Publishers, The Netherlands.

Kawaguchi, Y., et al., 1996, "Turbulent Transport Mechanism in a Drag Reducing Flow with Surfactant Additive Investigated by Two Component LDV", 8th Intl. Symp. on Appl.of Laser Techniques to Fluid Mechanics, July 8-11, Lisbon Portugal, II, pp. 29.4.1-29.4.7.

Kawaguchi, Y., et al., 1997a, "Existence of double disffusivity layers and heat transfer characteristics in drag reducing channel flow", Turbulence, Heat and Mass Transfer, pp. 157-166

Kawaguchi, Y., et al., 1997b, "Turbulence Characteristics in Transition Region of Dilute Surfactant Drag Reducing Flows", Proc. 11th Intl. Symp. Turbulent Shear Flows, Sep. Grenoble, France, pp. P1-49-P1-54.

Kevlahan, N.K.-R., 1993, "Rapid Distortion of Turbulent Structures", Appl. Sci. Research, 51, pp. 411-415

Li, P.W., Kawaguchi, Y. and Yabe, A., 1999, "Control of drag-reduction by channel height modification - transitional turbulent characteristics from drag-reducing flow to turbulent flow", Turbulence and Shear Flow-1, pp. 1339-1344, Begell house

Mysels, K.J., 1949, "Flow of Thickened Fluids", U.S. Patent 2,492,173, December 27.

Ohlendorf, D., Interthal, W. and Hoffmann, H., 1986, "Surfactant Systems for Drag Reduction: Physico-Chemical Properties and Rheological behavior", Rheol. Acta, Vol.25, pp. 468-486.

Pollert, J., Zakin, J.L., Myska, J. and Kratochivil, P., 1994, "Use of Friction Reducing Additives in District Heating System Field Test at Kladno-Krocehlavy, Czech Republic", Proc. 85th Int. District Heating and Cooling Assoc. Seattle, USA, pp. 141-156.

Toms, B.A., 1948, "Some Observation on the Flow of Linear Polymer Solutions Through Straight Tubes at Large Reynolds Numbers", Proc. 1st Intl. Congr. on Rheology, Vol. II, pp. 135-141, North Holland, Amsterdam.